International Journal of Biochemistry and Cell Biology 106 (2019) 74–83

Contents lists available at ScienceDirect

International Journal of Biochemistry and Cell Biology

journal homepage: www.elsevier.com/locate/biocel

RNA-binding proteins RBM20 and PTBP1 regulate the alternative splicing of *FHOD3*

Lorenzi P., Sangalli A., Fochi S., Dal Molin A., Malerba G., Zipeto D., Romanelli M.G.*

Department of Neurosciences, Biomedicine and Movement Sciences, Section of Biology and Genetics, University of Verona, Italy

ARTICLE INFO

Keywords:
RBM20
FHOD3
Alternative splicing
PTBP1
RRM
Sarcomere

ABSTRACT

Regulation of alternative splicing events is an essential step required for the expression of functional cytoskeleton and sarcomere proteins in cardiomyocytes. About 3% of idiopathic dilated cardiomyopathy cases present mutations in the RNA binding protein RBM20, a tissue specific regulator of alternative splicing. Transcripts expressed preferentially in skeletal and cardiac muscle, including *TTN*, *CAMK2D*, *LDB3*, *LMO7*, *PDLIM3*, *RTN4*, and *RYR2,* are RBM20-dependent splice variants. In the present study, we investigated the RBM20 involvement in post-transcriptional regulation of splicing variants expressed by Formin homology 2 domain containing 3 (*FHOD3)* gene. FHOD3 is a sarcomeric protein highly expressed in the cardiac tissue and required for the assembly of the contractile apparatus. Recently, *FHOD3* mutations have been found associated with heart diseases. We identified novel *FHOD*3 splicing variants differentially expressed in human tissues and provided evidences that *FHOD3* transcripts are specific RBM20 and PTBP1 targets. Furthermore, we demonstrated that the expression of RBM20 and PTBP1 promoted the alternative shift, from inclusion to exclusion, of selected FHOD3 exons. These results indicate that RBM20 and PTBP1 play a role in the actin filament functional organization mediated by *FHOD3* isoforms and suggest their possible involvement in heart diseases.

1. Introduction

Alternative splicing is a post-transcriptional process necessary for organ development, tissue organization, and cell differentiation. The recent applications of next-generation-sequencing technologies indicate that > 95% of human pre-mRNA transcribed by multi-exon genes undergo alternative splicing, enormously amplifying the expression potential of the human transcriptome (Wang et al., 2008; Wang and Burge, 2008; Nilsen and Graveley, 2010). Alternative splicing events are responsible for transcripts stability and distinct functions of the protein isoforms, involving a large repertoire of splicing factors (Wang et al., 2008; Nilsen and Graveley, 2010; Sahebi et al., 2016). A growing number of studies has explored the mechanisms of co- and post-transcriptional RNA splicing. However, the molecular basis of tissue-specific alternative splicing regulation and the properties of the splicing regulatory networks are still far from being fully understood. Given the complexity and frequency of the alternative splicing events, it is not surprising that genetic diseases, cancer, metabolic diseases, neurodegenerative and cardiovascular diseases may derive by aberrant splicing events or splicing mis-regulation (Daguenet et al., 2015; Chabot and Shkreta, 2016; Scotti and Swanson, 2016; Latorre and Harries, 2017; Saez et al., 2017).

Two distinct mechanisms may affect alternative splicing: 1) mutations of the consensus sequences for the splice sites or the auxiliary *cis*-regulatory sequence elements; 2) defects in the activity of the *trans*-regulators of alternative splicing events (Dames et al., 2011; Chabot and

Abbreviations: aa, amino acid; cDNA, complementary DNA; CUGBP1, CUG-binding protein 1; DCM, dilated cardiomyopathy; DID, diaphanous inhibitory domain; DMEM, Dulbecco's modified Eagles medium; FHOD3, formin homology 2 domain containing protein 3; GAPDH, GlycerAldeides-3-phosphate DeHydrogenase; GBD, GTPase-binding domain; GFP, green fluorescent protein; hnRNP, heterogeneous nuclear ribonucleoprotein; MBNL1, muscleblind-like protein 1; nPTB, neuronal polypyrimidine-tract binding protein; PCR, polymerase chain reaction; PTBP1, polypyrimidine-tract binding protein 1; RBM20, RNA binding motif protein 20; RIP, RNA ImmunoPrecipitation; RNP, RiboNucleoProtein; RRM, RNA Recognition Motif; RS, Arginine Serine domain; RT-PCR, reverse transcription polymerase chain reaction; RBFOX1, RNA binding protein fox-1 homolog 1; snRNPs, small nuclear ribonucleoproteins; TTN, Titin

* Corresponding author at: Department of Neurosciences, Biomedicine and Movement Sciences, Section of Biology and Genetics, University of Verona, Strada le Grazie 8, 37134, Verona, Italy.

E-mail addresses: pamela.lorenzi@univr.it (P. Lorenzi), antonella.sangalli@univr.it (A. Sangalli), stefania.fochi@univr.it (S. Fochi), anna.dalmolin.1@gmail.com (A. Dal Molin), giovanni.malerba@univr.it (G. Malerba), donato.zipeto@univr.it (D. Zipeto), mariagrazia.romanelli@univr.it (M.G. Romanelli).

https://doi.org/10.1016/j.biocel.2018.11.009
Received 28 June 2018; Received in revised form 29 October 2018; Accepted 19 November 2018
Available online 20 November 2018

Shkreta, 2016; Scotti and Swanson, 2016). The *trans*-regulatory factors are commonly divided in two classes: the Ser/Arg-rich (SR) proteins (Long and Caceres, 2009; Zhou and Fu, 2013) and the heterogeneous nuclear ribonucleoprotein (hnRNP) families (Martinez-Contreras et al., 2007). In general, SR proteins facilitate the exon inclusion in mature transcripts, whereas the hnRNP proteins participate to exon exclusion or skipping (House and Lynch, 2008; Wang and Burge, 2008). Synergistic and competitive interactions between different SR proteins and hnRNP are determinant in post-transcriptional control of alternative splicing during development and tissue differentiation. This is the case of the well-known alternative splicing regulators, the polypyrimidine tract-binding protein 1 (PTBP1) and its paralog PTBP2 that are differentially expressed during tissue differentiation leading to tissue specific alternative splicing (Zheng et al., 2012; Romanelli et al., 2013). The expression of PTBP1 in non-neuronal cell represses the neural-specific splicing program, whereas neural-specific splicing events occur during neurogenesis by PTBP1 down regulation and PTBP2 overexpression (Makeyev et al., 2007; Keppetipola et al., 2012; Vuong et al., 2016). As well as for neuronal development, RNA binding proteins are critical factors in heart development (Blech-Hermoni and Ladd, 2013). Recently, a direct role in cardiovascular disease has been attributed to the altered function of RNA-binding proteins that regulate splicing events (Lara-Pezzi et al., 2013; Weeland et al., 2015; van den Hoogenhof et al., 2016; De Bruin et al., 2017; Zhu et al., 2017). An interesting example is represented by the RNA–binding motif protein 20 (RBM20), a pre-mRNA splicing factor highly expressed in heart, whose mutations are associated with approximately 3% of the cases of dilated cardiomyopathy (DCM) (Aurora et al., 2007; Brauch et al., 2009; Li et al., 2010; Refaat et al., 2012). The ribonucleoprotein RBM20 is characterized by an RNA recognition motif (RRM) and a SR reach domain (Brauch et al., 2009), both required for nuclear localization (Filippello et al., 2013). Phosphorylation of the RS-rich region is critical for RBM20 nuclear localization (Murayama et al., 2018). RBM20 predominantly binds to intronic sequences containing an UCUU motif in close proximity to tissues regulated exons, acting as a splicing repressor (Guo et al., 2012; Li et al., 2013). Exons composition of 49 genes has been found to be RBM20-dependent (Guo et al., 2012; Maatz et al., 2014; Rexiati et al., 2018). This set of genes includes: the sarcomeric structural proteins *TTN* (titin), *LDB3* (PDZ-LIM domain-binding factor), and *PDLIM3* (PDZ and LIM Domain 3); the Ca^{2+} regulator *CAMK2D* (calcium/calmodulin dependent protein kinase II Delta); *LMO7* (LIM Domain Only 7) protein involved in adhesion junction formation; the endoplasmic reticulum associated protein *RTN4* (reticulon 4); the calcium - channel component of the cardiac muscle sarcoplasmic reticulum *RYR2* (Ryanodine Receptor 2) (Guo et al., 2012, 2013; Beraldi et al., 2014; Maatz et al., 2014). All these genes are required for diastolic function, sarcomere assembly and ion transport suggesting a relevant role of RBM20 in the molecular switch of tissues specific isoforms in cardiomyocytes. The role of RBM20 has been functionally validated for the alternative splicing of *TTN* and *Camk2d* (Guo et al., 2012; Li et al., 2013). Recently, an induced pluripotent stem cells model of familial DCM has been produced from dermal fibroblasts obtained by patients with an aggressive form of DCM owing to a missense mutation in exon 9 of RBM20. In this model the mis-splicing of LDB3, TTN and dysregulation of Ca^{2+} homeostasis have been reported (Wyles et al., 2016).

In the present study, we focused our analyses on the RBM20 role in post-transcriptional regulation of the formin homology 2 domain containing 3 (*FHOD3*) gene. The *FHOD3* transcripts have been previously included in the molecular target framework regulated by RBM20 (Guo et al., 2012), but it has not yet been validated as a direct RBM20-target of splicing regulation. FHOD3 is an actin–organizing protein that regulates the sarcomere organization in cardiomyocytes (Taniguchi et al., 2009). The protein belongs to the formin protein family, characterized by the presence of formin homology (FH) conserved sequences. FHOD3 contains three FH domains, a GTPase binding domain (GBD), a diaphanous autoinhibitory domain (DID) in the FH3 region and a diaphanous autoregulation domain (DAD) at the C-terminal (Schönichen and Geyer, 2010; Iskratsch et al., 2013). Intramolecular interaction between DID and DAD leads to FHOD3 dimerization that stimulates the synthesis of actin filaments (Li and Higgs, 2003; Kühn and Geyer, 2014). FHOD3 expression shows tissue specificity, being highly expressed in heart, kidney, and brain (Katoh and Katoh, 2004). Two major variants of FHOD3 have been identified: a long and a short isoform, FHOD3L and FHOD3S respectively, deriving by tissue-specific splicing in the region coding for the N-terminal of the protein. In human tissues they differ for an internal deletion of 453 nucleotides, resulting in a shorter FHOD3 isoform deleted of 151 amino acids in the FH3 domain. The FHOD3S isoform is predominantly expressed in kidney and brain, whereas the long isoform is mainly expressed in the heart (Kanaya et al., 2005). Further studies have identified a human muscle–specific isoform named $T(D/E)_5XE$ FHOD3 which is regulated in exon 26 and characterized by the insertion of eight additional amino acids at the C-terminal end of the FH2 domain. The translation of these amino acids introduces a phosphorylation site for casein kinase 2 (CK2) that affects the half-life of FHOD3 in cardiomyocytes (Iskratsch et al., 2010, 2013). This FHOD3 striate muscle-specific splice isoform promotes the polymerization of actin filaments in cardiomyocytes and is required for myofibrils and sarcomeric structure integrity (Taniguchi et al., 2009; Iskratsch et al., 2010). The requirement of FHOD3 in heart function is demonstrated in *Fhod3* knockout mice that present disturbed myofibril maturation and embryonic lethality due to defects in heart development. Furthermore, transgenic mice expressing a FHOD3 protein with a mutation in the FH2 domain are defective in actin-assembly activity and exhibit a cardiomyopathic phenotype (Kan-O et al., 2012a). In human, *FHOD3* mutations have been associated with hypertrophic cardiomyopathy (HCM) (Wooten et al., 2013) and DCM (Arimura et al., 2013). It may be expected that RBM20 expression modifies the FHOD3 splicing pattern, conditioning actin filaments polymerization. In order to investigate the involvement of RBM20 into FHOD3 post-transcriptional regulation, we analyzed its role in the expression pattern of alternative spliced FHOD3 transcripts. We demonstrated that the expression of both RBM20 and PTBP1 are associated with the expression of alternatively spliced FHOD3 transcripts. We propose that RBM20 mutations may affect sarcomere organization by altering the expression of cardiomyocyte-specific spliced isoforms of FHOD3 contributing to DCM.

2. Materials and methods

2.1. Cell cultures and transfection

Adherent HeLa cells were maintained in exponential growth in Dulbecco's modified Eagles medium (DMEM) (BioWhittaker), supplemented with 10% fetal bovine serum (FBS, Cambrex), glutamine (2.0 mM), penicillin (100 units/L), and streptomycin (100 mcg/L). Cell lines were maintained at 37 °C in the presence of 5% CO_2. Cells were grown to 80% confluence before transfection with plasmid DNA using the Turbofect™ transfection reagent (Thermo Scientific) according to the manufacturer's instructions. After 48 h, cells were harvested and lysed for RNA extraction, protein analysis by Western blotting and RNA-protein binding analysis. For over-expression experiments, increasing quantities of plasmids were used (i.e. 0.1μg, 1μg, 2μg).

2.2. Bioinformatics analysis

The *FHOD3* gene sequence was retrieved from the Ensembl site (http://www.ensembl.org; human genome reference sequence GRCh38, ENST00000590592.5). Exon regions were made up of the first and final 30 nucleotides and 200 flanking intronic nucleotides. Acceptor and donor splicing sites were predicted by BDGP splicing predictor (http://www.fruitfly.org/seq_tools/splice.html).

RBM20 RNA binding sites were searched along the target sequences using a nucleotide probability (np) matrix constructed from data reported by Maatz et al. (Maatz et al., 2014). For every position, the overall probability (i.e. score) to be a RBM20 RNA binding site was defined as the sum of the negative logarithm value of the recurrence of such nucleotide in the np matrix. The score values ranged from -44 to -1. Positions with the higher scores were more likely to be a RBM20 RNA binding site. A threshold of score > -3 was arbitrary used to tag the most likely RBM20 RNA binding sites.

Three different computational approaches have been used to map PTBP1 RNA binding sites: (1) a np matrix for PTBP1 sites found in literature (CUCUCU) (Oberstrass et al., 2005), (2) the RegRNA2.0 (UUCUCU, UCUUCUU), and (3) RBPmap (CUCUCU, UCUU) online tools (http://regrna2.mbc.nctu.edu.tw/index.html; http://rbpmap.technion.ac.il/) (Chang et al., 2013; Paz et al., 2014).

Only the positions with the highest scores, i.e. presenting a perfect match or only one mismatch with the searched PTBP1 motif, were selected.

2.3. Plasmids

The Human RBM20 GFP tagged construct was previously described (Filippello et al., 2013). The GFP-PTBP1 plasmid was prepared by cloning a cDNA fragment corresponding to the entire human PTBP1 coding sequence (NM_002819) obtained by HeLa cells in the pcDNA6.2/N-EmGFP vector (Invitrogen).

2.4. RT-PCR

RNA was purified from HeLa cells, using the TRIzol reagent (Invitrogen). Reverse transcription reactions were performed at 50 °C for 50' with the Superscript III Reverse Transcriptase (Invitrogen) and a combination of oligo(dT)20 and random hexamers. RT-PCR reactions were performed using the GoTaq® Green Master Mix (Promega). Primer pairs for CAPN3, EIF4G2, FHOD3, GAPDH, PTBP1, RBM20 and RYR2 are listed on Table 1. CAPN3 primer pair designed for the RIP assay amplifies a constitutive region of all CAPN3 transcripts. Primers F and R for EIF4G2 were previously described (Xue et al., 2009). FHOD3 F1 and R1 were used for splicing isoform analysis in different tissues and for the over-expression assay, while the FHOD3 F3-R2 pair was used for the RIP assay. PTBP1 F1 and R1 primers used for RIP assay were designed on exon 1-2 and 3-4 boundaries, respectively (Romanelli et al., 2000). In order to specifically amplify exogenous PTBP1 transcript, the plasmid-specific primer FP1 (Vivid Colors™ pcDNA™ 6.2/EmGFP Invitrogen) was used for RT-PCR in the overexpression assay, together with a primer complementary to a sequence in the PTBP1 exon 6 (PTBP1 R2). RBM20 primers were previously described (Filippello et al., 2013). RYR2 F1 and R1 for RIP assay were designed on exon 101 and 103, respectively. The RYR2 F2 R2 primer pair was designed on the human transcript according to the primers position relative to the rat orthologs previously described (Maatz et al., 2014). Human expression analysis was performed on six different tissues: heart, skeletal muscle, brain, pancreas, liver and kidney (Multiple Tissue cDNA panel I, BD Biosciences Clontech). Relative bands intensity was evaluated after gel electrophoresis using the Image J image processing program (https://imagej.nih.gov/ij/).

The sequences of the amplified bands were confirmed by sequencing at the BMR Genomics DNA Analysis Service. The non-parametric Kruskal–Wallis test by ranks was used for testing whether FHOD3 isoforms were expressed at different levels when undergoing RBM20 or PTBP1 transfection (the R package version 3.4.1 was used for the analysis; https://cran.r-project.org/).

2.5. Real -time PCR

Total RNA was transcribed to cDNA using SuperScript IV VILO Master Mix (Invitrogen) according to the manufacturer's instructions. Quantitative RT-PCR was performed with SsoAdvanced Universal SYBR Green Supermix (BioRad) on a CFX96Connect Real-Time System (BioRad). Primers for FHOD3 F (FHOD3 F5 and R4) and B (FHOD3 F4 and R3) variant transcripts were designed for spanning exon-exon junctions by PrimerQuest Tool (Integrated DNA Technologies https://eu.idtdna.com/site/account/login?returnurl=/Primerquest/Home/Index). TBP (Tata Box Binding Protein) was used as reference gene. All

Table 1
Primer pairs used for RT PCR.

Primer	Position[a]	Reference sequence	Primer sequence	Exon
CAPN3 F	2239-2260	NM_000070.2	GATCAGGAAAGTGAGGAACAGC	17
CAPN3 F	2402-2421	NM_000070.2	ATCCATGAGCGCAATCATGC	19
EIF4G2 F	1674-1693	NM_001418	ATCGCAGTTTGGAGAGATGG	13
EIF4G2 R	1956-1937	NM_001418	CTGTCCCAGAGGTGGTGTTT	15
FHOD3 F1	903-924	NM_001281740	GATGGAGTTGATACGGAGCTAC	8
FHOD3 F2	1351-1370	NM_001281740	AAGAGGAGCAGCCAATCACG	11
FHOD3 F3	4385-4407	NM_001281740	TTTACTCTTTATGGGCCATCCAC	25
FHOD3 F4	1704-1725	NM_001281740	CCCTTCCACCTCTTCTCCTAT	12
FHOD3 F5	1308-1325	NM_001281740	CCCAACCAAGTGCGAGAT	10
FHOD3 R1	1983-2003	NM_001281740	TGATGTGAGAAGACCACTCGG	15
FHOD3 R2	4544-4565	NM_001281740	ATCGGTGATCATCTTCCCTCTG	25
FHOD3 R3	1779-1877	NM_001281740	GCCAAAATTGCTGTATCTGTTTTC	12-14
FHOD3 R4	1418-1985	NM_001281740	CGGTGATGACCTGTCCTT	11-15
FP1	1594-1614	pcDNA™ 6.2/EmGFP	ACAAGGGCTCGAGCCCATCAA	–
GAPDH F	291-316	NM_001289745	TGAAGGTCGGAGTCAACGGATTTGGT	2-3
GAPDH R	1250-1273	NM_001289745	CATGTGGGCCATGAGGTCCACCAC	9
PTBP1 F1	1653-1667	NM_002819	CCGGAATCCGACGGCATTGTCCCA	1-2
PTBP1 R1	1775-1756	NM_002819	ATTTCCGTTTGCTGCAGAAG	3-4
PTBP1 R2	658-679	NM_002819	GAGGTTCTCCACGATGATCCTG	6
RBM20 F	1811-1830	NM_001134363	AAGTTGCTCATTCGGATGTC	7
RBM20R	2001-2019	NM_001134363	GAGGTGAAGCTGGGAGTGT	9
RYR2 F1	14684-14701	NM_001035	TTGTCATTCTCTTGGCCA	101
RYR2 F2	11225-11247	NM_001035	AGGAAGATGACGATGGTGAAGAG	80
RYR2 R1	14767-14785	NM_001035	AGCATTTGGTCTCCATGTC	102-3
RYR2 R2	11338-11358	NM_001035	GGCACTGATTGTCTGTAGCAC	81
TBP F	783-803	NM_003194	TGTATCCACAGTGAATCTTGG	4
TBP R	884-866	NM_003194	ATGATTACCGCAGCAAACC	5

[a] Position are relative to nucleotides numeration sequence reference mRNAs listed in "reference sequence" column.

primers sequences for real-time PCR are listed in Table 1. The comparative threshold cycle method (ΔΔCt) was used to quantify relative amounts of product transcripts. The specificity of amplicons was confirmed by melting-curve analysis. Each test was repeated in triplicate. Data are presented as mean ± SD. Z-score test of the log fold change was performed pairwise to compare control and treated samples.

2.6. RNA immunoprecipitation (RIP) assay

The RIP assay was performed on HeLa cells. Cells lysis was conducted according to Rinn et al (Rinn et al., 2007) with some modifications. Briefly, 2×10^7 cells were harvested by trypsinization, resuspended in PBS/Nuclear Isolation Buffer NIB (1.28 M sucrose, 40 mM Tris-HCl PH 7.5, 20 mM $MgCl_2$, 4% Triton X-100) in H_2O (1/1/3 in volume) and put on ice for 20 min. Nuclei were pelleted by centrifugation at 2500 *g* for 15 min and lysed as previously described (Li et al., 2013). Briefly, nuclear pellet was suspended in 1 ml of FA lysis buffer containing 1 mM ethylenediaminetetraacetic acid, 50 mM [(4-(2-hydroxyethyl)-1-piperazineethanesulfonic acid] (HEPES)–KOH (pH 7.5), 140 nM NaCl, 0.1% sodium deoxycholate (w/v), 1% Triton X-100 (v/v). The lysis buffer was supplemented with 100 U/ml of RNaseOUT (Invitrogen) and 1 × protease inhibitor cocktail (cOmplete™ EDTA-free Protease Inhibitor Cocktail Roche). After sonication and centrifugation at 15,000 *g* for 10 min at 4 °C, the supernatant was collected and first pre-cleared by an incubation with 15 µg of normal Rabbit IgG for 30' at 4 °C followed by an incubation with washed plain beads for 30' at 4 °C. The immunoprecipitation reaction was carried on by incubating the nuclear lysate over-night with the antibody-immobilized protein A Sepharose beads (anti-GFP antibody ChIP Grade Abcam or anti-PTBP1 RIP-certified antibody MBL and normal Rabbit IgG as a negative control). The FA buffer was used for washing the immunoprecipitated mRNP complexes; in the final wash, 2 M urea was added to FA. After protein digestion with proteinase K-SDS buffer, mRNAs were isolated from immunoprecipitated mRNPs with the TRIzol reagent (Invitrogen).

2.7. Western blot analysis of PTBP1 and RBM20 expression

HeLa cells transfected with GFP-PTBP1 or GFP-RBM20 expressing vectors were lysed in a non-denaturing lysis buffer (10 mM Tris-HCl, pH 7.5, 5 mM EDTA, 150 mM NaCl, 1% Triton X-100) with the addition of cOmplete™ EDTA-free Protease Inhibitor Cocktail (Roche). Protein samples were resolved on 12% or 8% SDS-PAGE followed by Western blotting using anti-RBM20 (bs-9606 r, Bioss), or anti-PTBP1 (RN011 P, MBL), or anti-GFP ChIP Grade (ab290, abcam) antibodies. HRP-conjugated anti-mouse (Sigma-Aldrich) or anti-rabbit (Thermo Scientific) IgG were used as secondary antibodies. The signal was developed using the ECL™ Prime Western blotting Detection Reagent (GE Healthcare), according to manufacturer's instructions, and collected by the ChemiDoc™ XRS + System (Bio-Rad).

3. Results

3.1. FHOD3 exons 11–14 are alternatively spliced

Based on a previous study that identified a specific FHOD3 isoform derived by N-terminal alternative splicing of exon 11 and 12 in mice heart tissues (Iskratsch et al., 2010), we decided to investigate whether a similar N-terminal alternative splicing occurred in human tissues. The FHOD3 human gene is organized in 29 exons expressing a full-length protein of 1622 amino acids (FHOD3 exons – introns structure derived by accession no. NM_001281740.2, NC_000018.10 and functional domains of the translated protein are represented in Fig. 1, panel a). During the analysis of tissue expressed FHOD3 transcripts, we identified novel exons alternatively spliced. PCR analyses with primers targeting exons 11 and 15 (Fig. 1, panel c), identified a differentially expressed pattern of transcripts, derived by the alternative splicing and corresponding to at least six isoforms, identified as A to F (Fig. 1, panel b). Based on the deducted size bands and direct sequencing of the more represented bands, we attributed to each band the alternative splicing of the exons 12, 13 and 14 as represented in Fig. 1 panel c. FHOD3 mRNAs containing exons 12–13 and 14 (A) were highly expressed in the heart and in the skeletal muscle and less abundantly in pancreas and liver. The long and short FHOD3 transcripts were also detected in HeLa cells. The results confirmed that FHOD3 isoforms containing exon 12 were expressed preferentially in heart and skeletal muscle, whereas in brain, pancreas, liver and kidney the shorter isoforms, derived by skipping of exons 12, were more expressed. A short isoform lacking exons 12 and 13 (isoform D) was preferentially expressed in brain, pancreas, liver, kidney, and HeLa cells. All the isoforms that may derive by the alternative splicing of exons 12, 13, and 14 did not insert in frame stop codons and may be potentially translated in shorter protein isoforms deleted in the FH3 domain of 120, 25 and 38 aa, respectively.

Taken together, our results indicate that FHOD3 may be expressed in several isoforms, which differ for the extension of the FH3 domain at its N-terminal end, involving exons 12, 13, and 14.

3.2. FHOD3 transcripts are RBM20 and PTBP1 target

Searching for similarity with FH3 domains present in orthologs formin families the sequences coded by exons 13 and 14 resulted to match only with FHOD3 isoforms. The 38 amino acids encoded by exon 14 were conserved in several paralogs identified in the genome databases, whereas the 25 amino acids codified by exon 13 were less represented and absent in both mouse and rat (Fig. 2, panel a).

In order to deepen the understanding of the alternative splicing regulation of exons 13 and 14 in FHOD3 messengers, we performed a bioinformatics analysis of the intronic flanking sequences, searching for known alternative splicing *cis*-acting patterns recognized by the ubiquitous splicing factor PTBP1 and/or by the tissues specific splicing factor RBM20. Patterns were searched across the regulated region (i.e. from exon 11 to exon 15) and in an arbitrary selected region not supposed to be regulated by PTBP1 or RBM20 (from exon 4 to exon 8) as negative control.

Several putative RBM20 RNA binding sites were identified in all the analyzed regions (Fig. 2, panel b) (as described in material and methods). Exons 12-14 flanking regions resulted to be enriched in putative binding sites compared to exons 5-7 flanking regions (24 and 16 binding sites, respectively), with a higher number of binding sites in exon 13 and exon 14 flanking regions. Moreover, exons 12-14 flanking regions presented a three-fold enrichment of overlapping sites for RBM20 than exons 5-7 flanking regions (9 and 3 groups of overlapping sites, respectively). When searching for the putative PTBP1 binding sites, the frequency and distribution were similar to the frequency and distribution of RBM20 consensus sites: exons 12-14 flanking regions showed a higher number of binding sites compared to exons 5-7 flanking regions (28 and 16 binding sites, respectively), with exons 13 and 14 flanking regions enriched in binding sites. Exons 11-15 compared to exons 4-8 regions showed 10 versus 7 groups of overlapping sites for PTBP1.

To confirm that RBM20 binds to FHOD3 RNA, we performed the RNA immunoprecipitation assay (RIP). HeLa cells that do not express RBM20 (Filippello et al., 2013) were transfected with a GFP-RBM20 plasmid and the enriched RNA present in the anti-GFP immunocomplexes was analyzed by RT-PCR. The cDNAs produced by the immunoprecipitated RNA were amplified with specific primers, recognizing exons 11, 15 and 25 of FHOD3. The enrichment of RNA specific targets of RBM20 was confirmed by amplification of RYR2 transcripts, known to be recognized by RBM20 (Maatz et al., 2014) and using negative controls represented by PTBP1 and GAPDH transcripts which are expected not to bind RBM20. The results showed that FHOD3 transcripts may be amplified by the ribonucleoproteins complexes containing RBM20 (Fig. 3, panel a). Control immunoprecipitation with

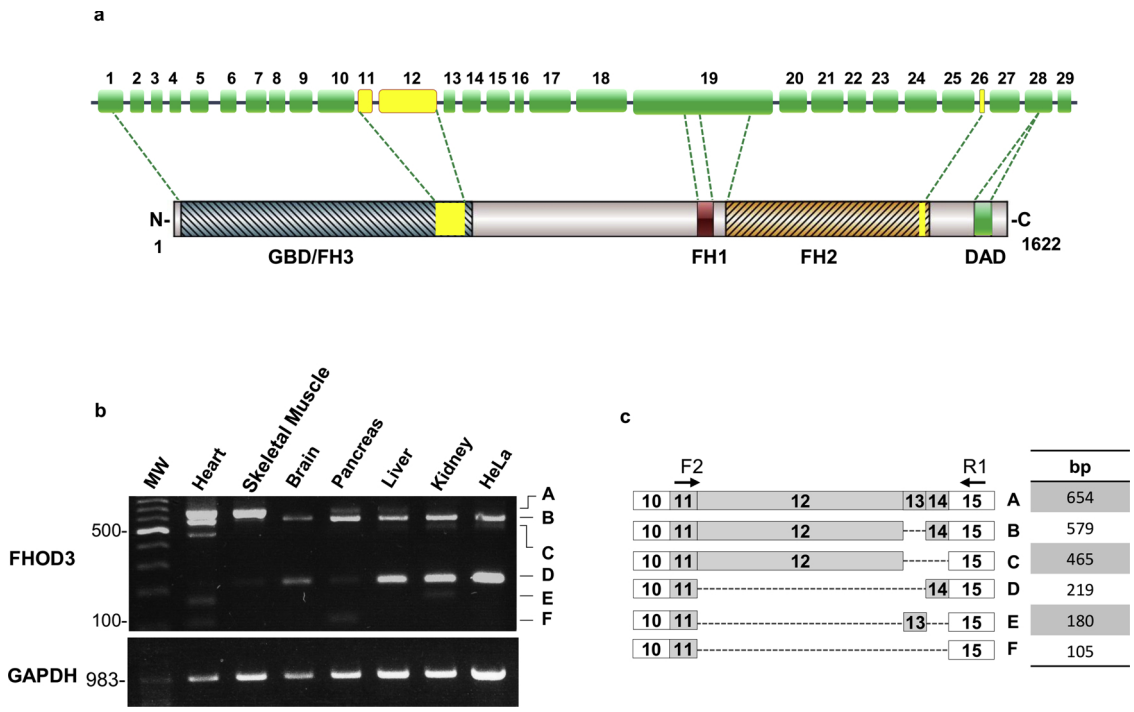

Fig. 1. FHOD3 splicing variants. (a) Human FHOD3 gene organization and protein domains. GBD, GTPase-Binding Domain; FH1, FH2 and FH3, Formin Homology domains; DAD Diaphanous Autoregolatory Domain. (b) FHOD3 transcripts expression analysis performed by RT-PCR on six different human tissues and HeLa cells. (c) Representation of exons organization in FHOD3 variants (A to F) in the region encompassing exons 8–15. The expected sizes are indicated in the table.

pre-immune IgGs (mock) gave no enrichment in any of the mRNAs analyzed. Immuno-precipitation with specific antibody (anti-GFP) from transfected cells and western blot analysis revealed the presence of RBM20 protein. Further, we performed the RIP assay from HeLa cells using a specific PTBP1 antibody. The enriched RNA were analyzed by RT-PCR with specific primers that recognized the CAPN3 (calpain 3) and PTBP1 transcripts, known to be PTBP1 target (Wollerton et al., 2004; Boutz et al., 2007) and FHOD3 primers. GAPDH primers were used as a negative control. FHOD3 transcripts were amplified by the RNA present in the immunocomplexes containing PTBP1 (Fig. 3, panel

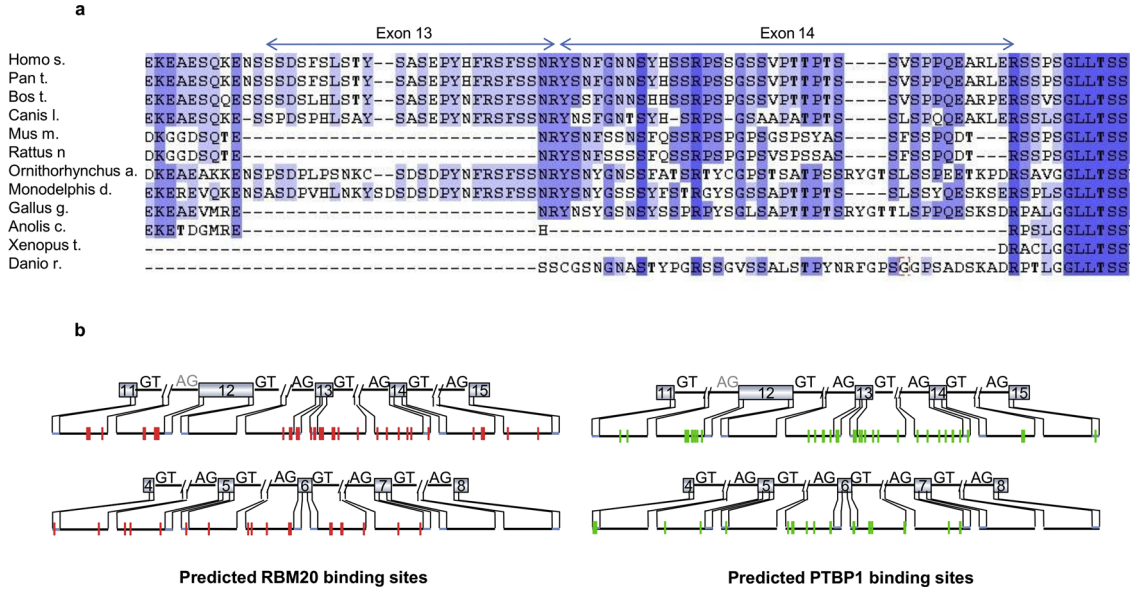

Fig. 2. Computational analysis of amino acids homology and intron-exon distribution of *cis*- regulatory sequences for RBM20 and PTBP1. (a) Deduced amino acid sequences encoded by the alternative spliced human exons 13 and 14 in comparison with orthologs. Amino acid sequences were aligned with the MafftWs multiple sequence alignment program and drawn with Jalview multiple sequence alignment editor http://www.jalview.org (Waterhouse et al., 2009). Color intensity indicates the percentage of the residues in each column in agreement with the consensus sequence. (b) Positions of the predicted RBM20 (red vertical lines) and PTBP1 (green vertical lines) RNA binding sites present in 230 nucleotides (nt) regions (30 nt inside the exon and 200 nt adjacent the exon) relative to exons 12, 13, 14, and exons 5, 6, 7 of FHOD3 human gene. Exons are shown as blue squares, and introns as black horizontal lines. "GT" and "AG", indicating the splicing sites according to BDGP splicing predictor, are reported in black or gray when detected or not, respectively. A single putative RNA binding site is represented by a thin vertical line, a single group of putative overlapping sites by a line whose width is proportional to the size of the region (For interpretation of the references to colour in this figure legend, the reader is referred to the web version of this article).

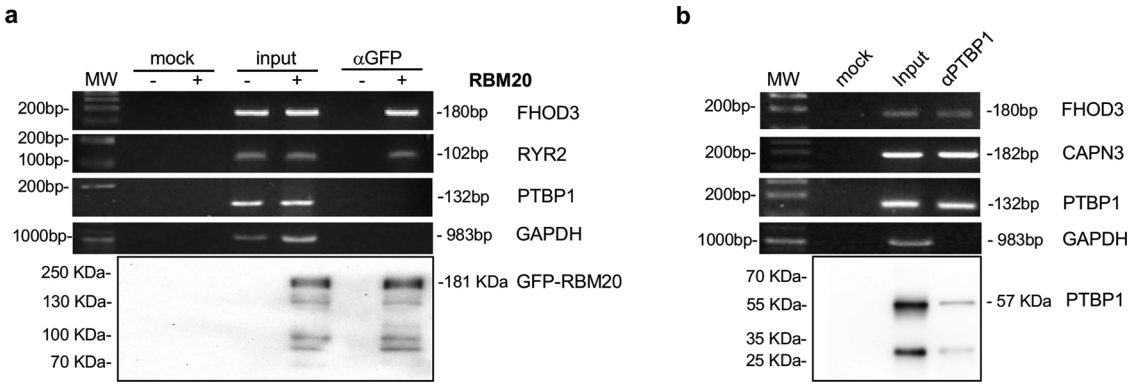

Fig. 3. Identification of RBM20 and PTBP1 mRNA targets by RNA immunoprecipitation analysis. (a) RT-PCR on RNA immunoprecipitated with the RBM20 antibody; the top panel shows the amplification signal obtained with FHOD3 (F3-R2), RYR2 (F1-R1), PTBP1(F1-R1) and GAPDH (F–R) specific primers. (b) RT-PCR on RNA immunoprecipitated with the PTBP1 antibody; the top panel shows the amplification signal obtained with FHOD3 (F3-R2), CAPN3 (F–R), PTBP1 (F1-R1), GAPDH (F–R). An aliquot of the immunoprecipitated RNPs was analyzed by western blot for the presence of RBM20 or PTBP1 proteins. Input: precleared cell lysate; mock: post immunoprecipitation beads coated with Rabbit IgG; αGFP: post immunoprecipitated beads coated with anti GFP polyclonal antibody; αPTBP1: post- immunoprecipitated beads coated with anti PTBP1 polyclonal antibody; - untransfected cells, + GFP-RBM20 plasmid transfected cells.

b). These results confirmed that both RBM20 and PTBP1 bind to FHOD3 mRNA and, thus, participate to the processing of FHOD3 transcript.

3.3. RBM20 and PTBP1 overexpression causes a shift of alternative splicing pattern of FHOD3 transcripts

A semiquantitative RT-PCR approach was used to address the effect of RBM20 over expression on FHOD3 expression pattern of alternatively-spliced transcripts. HeLa cells were transfected with increasing amount of the GFP-RBM20 expressing vector and transcripts were analyzed by RT-PCR (Fig. 4, panel a). The expression of FHOD3 transcripts was normalized to GAPDH and statistically analyzed in three independent replicates of RBM20 overexpression (box plot in Fig. 4, panel b). The results of the correlation analyses showed that the expression of the FHOD3 short isoform lacking exons 12-13-14 (isoform F) was more represented ($p = 0.00047$) in the presence of increased amounts of RBM20, whereas no significant variations were observed for the longer isoforms B (Fig. 4, panels a and b). Similar correlation analyses were performed comparing the expression of two additional genes regulated by alternative splicing: RYR2, which is known to be regulated by RBM20 (Maatz et al., 2014) and EIF4G2 (Eukaryotic Translation Initiation Factor 4 Gamma 2), regulated by PTBP1 (Xue et al., 2009). We did not observe significant differences in the spliced variants of RYR2 and EIF4G2 analyzed (Fig. 4, panel a). Further semiquantitative analyses were performed to compare FHOD3 variants expression levels to PTBP1 overexpression. Interestingly, we observed a highly significant difference ($p = 1{,}77 \times 10^{-5}$) in the expression pattern of the isoform F, as shown in the correlation analyses with RBM20 overexpression (Fig. 4, panels d, e). A significant increase of the isoform F in the presence of overexpressed RBM20 or PTBP1 was confirmed by quantitative PCR (qPCR) analyses (Fig. 4, panel c and f). These results indicate that both RBM20 and PTBP1 are involved in the FHOD3 transcript variants expression.

4. Discussion

In the present study, we investigated the alternative splicing regulation by RBM20 protein of FHOD3 pre-mRNA and showed that RBM20 and PTBP1 expression influences the balance of the splicing pattern of FHOD3, promoting skipping of exons 12, 13 and 14. Many splicing factors play important roles in tissue-specific or developmentally regulated alternative splicing events. The identification of RBM20 as a hearth tissues specific splicing factor has provided new insights into the mechanism of heart disease progression. RBM20 mutations lead to aberrant alternative splicing of isoforms that are strictly linked to cardiac function (Rexiati et al., 2018). TTN, a giant multifunctional protein required for sarcomere integrity, is one of the RNA targets for which RBM20 role in the alternative splicing has been well characterized (Guo et al., 2012; Li et al., 2013; Chen et al., 2018; Guo et al., 2018). RBM20 represses, in a dose-dependent fashion, the splicing of selected exons in TTN pre-mRNA by binding to UCUU-containing RNA elements (Li et al., 2013; Maatz et al., 2014) leading to the expression of the TTN cardiac isoforms. RBM20 has been recently proposed as a potential target for pharmacological intervention in cardiomyopathy because of its ability to regulate TTN isoforms switching (Guo and Sun, 2018). For most of the RBM20 RNA targets recently identified (Guo et al., 2012; Maatz et al., 2014) the RBM20 role in the alternative splicing is largely unknown. In the list of genes for which the alternative splicing has been previously indicated as RBM20-dependent, we choosed to analyze the expression pattern of alternatively spliced isoforms of FHOD3 in the presence of different amounts of RBM20. We first selected a set of regulated FHOD3 exons and identified novel human FHOD3 isoforms that show a different tissue expression pattern. These isoforms include the previously described long and short FHOD3 variants (FHOD3L and FHOD3S) and the results confirm that the longer FHOD3 isoform is preferentially expressed in cardiac and skeletal muscle (Kanaya et al., 2005). In addition to these isoforms, we detected new FHOD3 alternative spliced isoforms in which exons 13 and 14 are regulated. The isoforms that include exon 13 and 14 present an elongated FH3 protein domain. The predicted translated sequences derived by exon 13 is not conserved in the formin family proteins and is absent from the rat and mouse FHOD3 orthologos suggesting a divergent evolution in the conservation of the residues required for the formin domains properties.

By RIP assay, we demonstrate that FHOD3 mRNAs are present in RBM20 immunocomplexes. These results confirm previous data that identified FHOD3 in the RBM20-dependent gene network (Guo et al., 2012). Interestingly, we found that immunocomplexes containing PTBP1 were enriched in FHOD3 transcripts. These results are in agreement with the computational analysis that identifies overlapping consensus sequences for RBM20 and PTBP1 in the regions flanking the FHOD3 regulated exons. The distribution of these sequences is compatible with the molecular mechanism of alternative splicing regulation demonstrated for PTBP1 and RBM20. PTBP1 binds to the intronic polypyrimidine tract containing CU-rich RNA elements, inducing RNA looping and alternative exon sequestration from the splicing machinery (Chou et al., 2000; Wagner and Garcia-Blanco, 2001; Amir-Ahmady et al., 2005), while RBM20 binds to UCUU-containing RNA elements repressing exon splicing (Li et al., 2013; Maatz et al., 2014). RBM20 binding site sequence occurs many times along the exon flanking

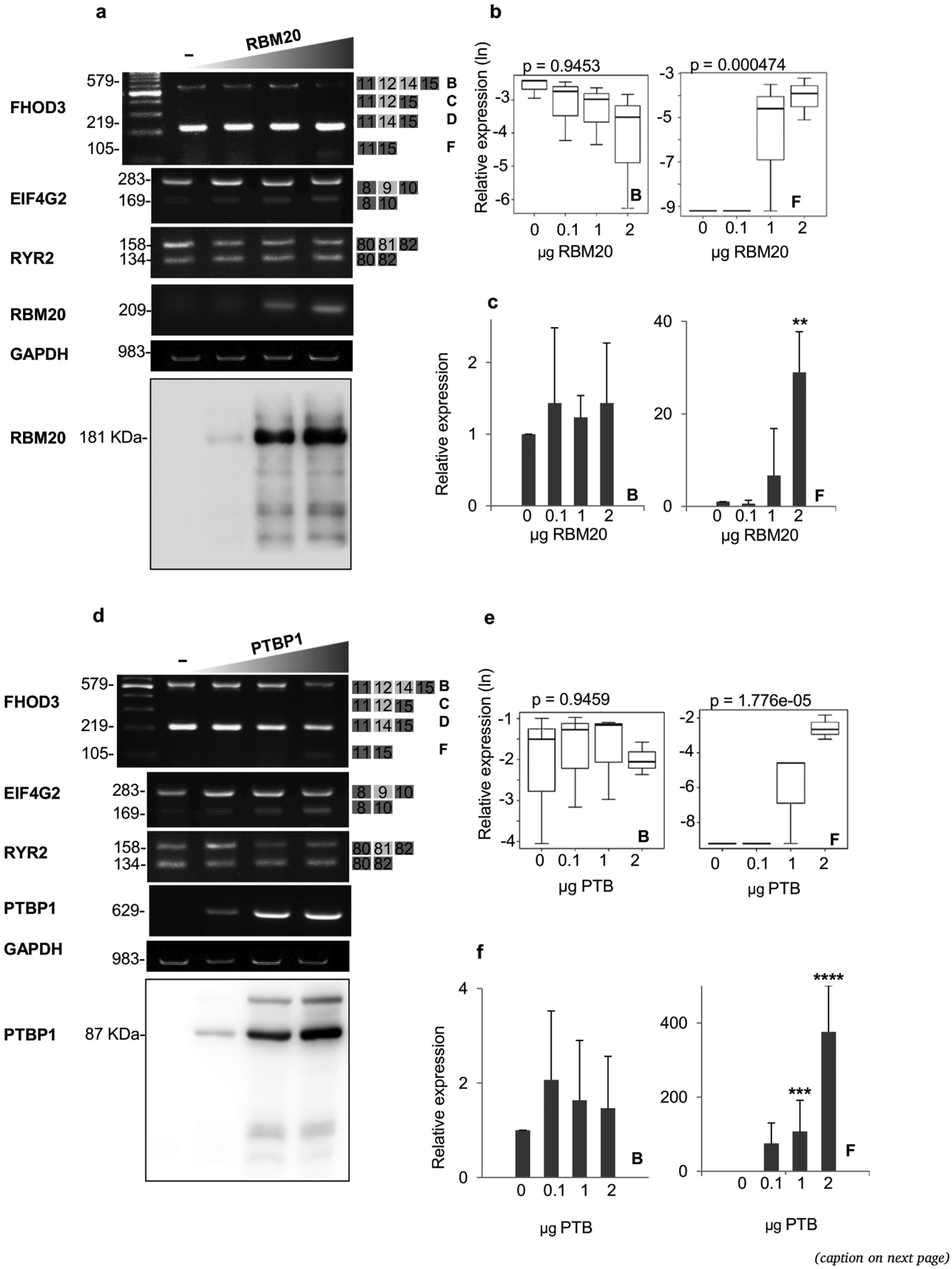

(caption on next page)

Fig. 4. RBM20 and PTBP1 overexpression modifies the alternative splicing patter of FHOD3 transcript expression. RT-PCR analysis of FHOD3 mRNA derived by HeLa cells transfected with increasing amounts (0.1, 1 and 2 μg) of GFP-RBM20 plasmid (a) or GFP-PTBP1 plasmid (d). Primers were selected to amplify FHOD3 region encompassing exon 11 to exon 15, EIF4G2 exon 8 to exon 10, RYR2 exon 80 to exon 81, RBM20 exon 7 to exon 9. Bottom panel: western blot of RBM20 and PTBP1 protein expression. Semi-quantitative FHOD3 B and F isoforms analysis in the presence of RBM20 (b) and PTBP1 (e). The evaluation of the relative intensity of PCR products was performed by image analysis using the Image *J* software. The box plots show the integrated optical density of isoforms bands normalized to GAPDH. The plot highlights the median (center line), maximum and minimum (whiskers, the vertical line), and 25 and 75% percentiles (boxes) of the data. The results are representative of three independent RT-PCR experiments. Quantitative FHOD3 B and F isoforms RT-PCR analysis in the presence of RBM20 (c) and PTBP1 (f). Fold change mRNA levels are compared to untrasfected HeLa cells. The results are presented as mean ± SD of three independent QPCR experiments. ** $0.001 < p < 0.01$, *** $0.0001 < p < 0.001$, **** $p < 0.0001$.

regions in FHOD3 pre-mRNA, with a higher frequency for exons 12, 13 and 14 flanking regions. The analogous search for PTBP1 RNA binding sites shows a similar result, suggesting a possible interaction of the two proteins in the regulation of the splicing of these exons. While we were preparing the manuscript, an interesting paper was published demonstrating that the regulation of TTN exons exclusion involves RBM20 and PTBP1 (alias PTB4). In this study the authors showed that RBM20 and PTBP1 bind to the same motive in the downstream intronic region of the TTN alternative exon 242 and proposed a model in which RBM20 and PTBP1 mechanistically compete to antagonize the effect on exon exclusion (Dauksaite and Gotthardt, 2018). We found that the overexpression of RBM20 or PTBP1 modified the alternative splicing patterns of FHOD3 transcripts. Notably, we observed a correlation between exon 12 skipping and the overexpression of RBM20 or PTBP1. We speculate that they both participate in the splice site recognition, possibly by competing with snRNP spliceosomal components and subsequently determining the exons inclusion/exclusion outcome. The alternative exons 12-13 and 14 are part of the GBD-FH3 domain that is responsible for stress fiber association and co-localization with myosin (Schulze et al., 2014), contributing to actin-assembly activity of FHOD3. In a study conducted in mice heart embryos the alternative exons 11 and 12 were demonstrated to be essential for the sarcomere localization of FHOD3, highlighting the relevance of a fine control of differentially expressed exons during heart development (Kan-O et al., 2012b). Our results attribute to RBM20 and PTBP1 a role in driving the tissues selection of the FHOD3 isoforms that may be required for the heart function. Several splicing factors are known to be involved in heart development and splicing of sarcomeric genes (Weeland et al., 2015; van den Hoogenhof et al., 2016; Zhu et al., 2017; Rexiati et al., 2018). RBM20 is the first splicing factor for which mutations have been associated to familial DCM. Other muscle-specific splicing factors have been associated with heart function and cardiomyopathy. These include: RBM24, an RNA binding protein containing the RRM motif, which is essential for heart development (Poon et al., 2012; Yang et al., 2014); the RNA binding protein fox-1 homolog1 (RBFOX1) that is involved in cardiac hypertrophy and heart failure (Pedrotti et al., 2015; Gao et al., 2016); the Muscleblind-like protein 1 (MBNL1) and CUG-binding protein 1 (CUGBP1) that lead to altered mRNA splicing associated to myotonic dystrophy type 1 (DM1) pathology when their expression is deregulated and unbalanced (Lin et al., 2006; Wang et al., 2007; Koshelev et al., 2010) the splicing factor SF3B1 that has been shown to be overexpressed in human heart diseases causing a shift in the ketohexokinase isoforms expressed in the cardyomyocites and altering the fructose metabolism regulatory system (Mirtschink et al., 2015). Recently it has been shown that, the co-expression of both RBM20 and RBM24 represses the hypertrophic remodeling of rat cardiomyocytes (Ito et al., 2016). In this model, RBM20 and RBM24 together promote the expression of the scaffold protein PDZ-LIM ENH3 (Enigma Homolog) isoforms preventing cardiomyocyte hypertrophy. It would be of interest to investigate whether PTBP1 may regulated *ENH* splice variants expression. In the heart, the aberrant alternative splicing is an emerging mechanism to be associated with cardiomyopathies (Song et al., 2012). RBM20 is the only identified splicing factor whose mutations, altering the RNA binding capability have been associated with human cardiomyopathy. The unbalanced splicing regulation derived by mutations in RBM20 and PTBP1 expression may affect FHOD3 as well as other RNA targets. Identifying the isoforms that are regulated by RBM20 in concert with PTB1 may contribute to best define the therapeutic strategies developed to rescue alternative splicing defects in human diseases including cardiomyopathies.

5. Conclusion

In this study, we identified PTBP1 as a novel FHOD3 splicing regulator. We have shown that both RBM20 and PTBP1 may contribute to the expression of FHOD3 isoforms, thus participating in actin assembly and sarcomeric organization in cardiomyocytes.

Additional functional studies on FHOD3 might help to understand the exact contribution of the described variants to the cardiomyocytes function and would provide significant new insights into the molecular mechanisms of heart function and disease.

Author contributions

PL, AS and SF performed the study and contributed to paper discussion and drafting; DZ, provided intellectual input and contributed to manuscript drafting; ADM and GM provided bioinformatics analysis; MGR conceived and designed the experiments, coordinated the study and contributed to paper drafting and writing. All authors read and approved the final manuscript.

Competing financial interest

The authors declare no competing financial interests.

Acknowledgment

This study was supported by grants from University of Verona, Italy (FUR Romanelli).

References

AMIR-AHMADY, B., Boutz, P.L., Markovtsov, V., Phillips, M.L., Black, D.L., 2005. Exon repression by polypyrimidine tract binding protein. RNA 11, 699–716. https://doi.org/10.1261/rna.2250405.

Arimura, T., Takeya, R., Ishikawa, T., Yamano, T., Matsuo, A., Tatsumi, T., Nomura, T., Sumimoto, H., Kimura, A., 2013. Dilated cardiomyopathy-associated FHOD3 variant impairs the ability to induce activation of transcription factor serum response factor. Circ. J. 77, 2990–2996.

Aurora, P., Boucek, M.M., Christie, J., Dobbels, F., Edwards, L.B., Keck, B.M., Rahmel, A.O., Taylor, D.O., Trulock, E.P., Hertz, M.I., 2007. Registry of the International Society for Heart and Lung Transplantation: Tenth Official Pediatric Lung and Heart/Lung Transplantation report—2007. J. Heart Lung Transplant. 26, 1223–1228. https://doi.org/10.1016/j.healun.2007.07.035.

Beraldi, R., Li, X., Martinez Fernandez, A., Reyes, S., Secreto, F., Terzic, A., Olson, T.M., Nelson, T.J., 2014. Rbm20-deficient cardiogenesis reveals early disruption of RNA processing and sarcomere remodeling establishing a developmental etiology for dilated cardiomyopathy. Hum. Mol. Genet. 23, 3779–3791. https://doi.org/10.1093/hmg/ddu091.

Blech-Hermoni, Y., Ladd, A.N., 2013. RNA binding proteins in the regulation of heart development. Int. J. Biochem. Cell Biol. 45, 2467–2478. https://doi.org/10.1016/j.biocel.2013.08.008.

Boutz, P.L., Chawla, G., Stoilov, P., Black, D.L., 2007. MicroRNAs regulate the expression of the alternative splicing factor nPTB during muscle development. Genes Dev. 21, 71–84. https://doi.org/10.1101/gad.1500707.

Brauch, K.M., Karst, M.L., Herron, K.J., de Andrade, M., Pellikka, P.A., Rodeheffer, R.J., Michels, V.V., Olson, T.M., 2009. Mutations in ribonucleic acid binding protein gene cause familial dilated cardiomyopathy. J. Am. Coll. Cardiol. 54, 930–941. https://

doi.org/10.1016/j.jacc.2009.05.038.
Chabot, B., Shkreta, L., 2016. Defective control of pre–messenger RNA splicing in human disease. J. Cell Biol. 212, 13–27. https://doi.org/10.1083/jcb.201510032.
Chang, T.-H., Huang, H.-Y., Hsu, J.B.-K., Weng, S.-L., Horng, J.-T., Huang, H.-D., 2013. An enhanced computational platform for investigating the roles of regulatory RNA and for identifying functional RNA motifs. BMC Bioinform. 14 (Suppl 2), S4. https://doi.org/10.1186/1471-2105-14-S2-S4.
Chen, Z., Song, J., Chen, L., Zhu, C., Cai, H., Sun, M., Stern, A., Mozdziak, P., Ge, Y., Means, W.J., Guo, W., 2018. Characterization of TTN Novex splicing variants across species and the role of RBM20 in novex-specific exon splicing. Genes (Basel) 9, 86. https://doi.org/10.3390/genes9020086.
Chou, M.Y., Underwood, J.G., Nikolic, J., Luu, M.H., Black, D.L., 2000. Multisite RNA binding and release of polypyrimidine tract binding protein during the regulation of c-src neural-specific splicing. Mol. Cell. 5, 949–957.
Daguenet, E., Dujardin, G., Valcarcel, J., 2015. The pathogenicity of splicing defects: mechanistic insights into pre-mRNA processing inform novel therapeutic approaches. EMBO Rep. 16, 1640–1655. https://doi.org/10.15252/embr.201541116.
Dames, S.A., Junemann, A., Sass, H.J., Schönichen, A., Stopschinski, B.E., Grzesiek, S., Faix, J., Geyer, M., 2011. Structure, dynamics, lipid binding, and physiological relevance of the putative GTPase-binding domain of dictyostelium formin C. J. Biol. Chem. 286, 36907–36920. https://doi.org/10.1074/jbc.M111.225052.
Dauksaite, V., Gotthardt, M., 2018. Molecular basis of titin exon exclusion by RBM20 and the novel titin splice regulator PTB4. Nucleic Acids Res. 46, 5227–5238. https://doi.org/10.1093/nar/gky165.
De Bruin, R.G., Rabelink, T.J., Van Zonneveld, A.J., Van Der Veer, E.P., 2017. Emerging roles for RNA-binding proteins as effectors and regulators of cardiovascular disease. Eur. Heart J. https://doi.org/10.1093/eurheartj/ehw567.
Filippello, A., Lorenzi, P., Bergamo, E., Romanelli, M.G., 2013. Identification of nuclear retention domains in the RBM20 protein. FEBS Lett. 587, 2989–2995. https://doi.org/10.1016/j.febslet.2013.07.018.
Gao, C., Ren, S., Lee, J.-H., Qiu, J., Chapski, D.J., Rau, C.D., Zhou, Y., Abdellatif, M., Nakano, A., Vondriska, T.M., Xiao, X., Fu, X.-D., Chen, J.-N., Wang, Y., 2016. RBFox1-mediated RNA splicing regulates cardiac hypertrophy and heart failure. J. Clin. Invest. 126, 195–206. https://doi.org/10.1172/JCI84015.
Guo, W., Sun, M., 2018. RBM20, a potential target for treatment of cardiomyopathy via titin isoform switching. Biophys. Rev. 10, 15–25. https://doi.org/10.1007/s12551-017-0267-5.
Guo, W., Schafer, S., Greaser, M.L., Radke, M.H., Liss, M., Govindarajan, T., Maatz, H., Schulz, H., Li, S., Parrish, A.M., Dauksaite, V., Vakeel, P., Klaassen, S., Gerull, B., Thierfelder, L., Regitz-Zagrosek, V., Hacker, T.A., Saupe, K.W., Dec, G.W., Ellinor, P.T., MacRae, C.A., Spallek, B., Fischer, R., Perrot, A., Özcelik, C., Saar, K., Hubner, N., Gotthardt, M., 2012. RBM20, a gene for hereditary cardiomyopathy, regulates titin splicing. Nat. Med. 18, 766–773. https://doi.org/10.1038/nm.2693.
Guo, W., Pleitner, J.M., Saupe, K.W., Greaser, M.L., 2013. Pathophysiological defects and transcriptional profiling in the RBM20 -/- rat model. PLoS One 8, e84281. https://doi.org/10.1371/journal.pone.0084281.
Guo, W., Zhu, C., Yin, Z., Wang, Q., Sun, M., Cao, H., Greaser, M.L., 2018. Splicing factor RBM20 regulates transcriptional network of titin associated and calcium handling genes in the heart. Int. J. Biol. Sci. 14, 369–380. https://doi.org/10.7150/ijbs.24117.
House, A.E., Lynch, K.W., 2008. Regulation of alternative splicing: more than just the ABCs. J. Biol. Chem. 283, 1217–1221. https://doi.org/10.1074/jbc.R700031200.
Iskratsch, T., Lange, S., Dwyer, J., Kho, A.L., dos Remedios, C., Ehler, E., 2010. Formin follows function: a muscle-specific isoform of FHOD3 is regulated by CK2 phosphorylation and promotes myofibril maintenance. J. Cell Biol. 191, 1159–1172. https://doi.org/10.1083/jcb.201005060.
Iskratsch, T., Reijntjes, S., Dwyer, J., Toselli, P., Dégano, I.R., Dominguez, I., Ehler, E., 2013. Two distinct phosphorylation events govern the function of muscle FHOD3. Cell. Mol. Life Sci. 70, 893–908. https://doi.org/10.1007/s00018-012-1154-7.
Ito, J., Iijima, M., Yoshimoto, N., Niimi, T., Kuroda, S., Maturana, A.D., 2016. RBM20 and RBM24 cooperatively promote the expression of short enh splice variants. FEBS Lett. 590, 2262–2274. https://doi.org/10.1002/1873-3468.12251.
Kanaya, H., Takeya, R., Takeuchi, K., Watanabe, N., Jing, N., Sumimoto, H., 2005. Fhos2, a novel formin-related actin-organizing protein, probably associates with the nestin intermediate filament. Genes Cells 10, 665–678. https://doi.org/10.1111/j.1365-2443.2005.00867.x.
Kan-O, M., Takeya, R., Abe, T., Kitajima, N., Nishida, M., Tominaga, R., Kurose, H., Sumimoto, H., 2012a. Mammalian formin Fhod3 plays an essential role in cardiogenesis by organizing myofibrillogenesis. Biol. Open. 1, 889–896. https://doi.org/10.1242/bio.20121370.
Kan-O, M., Takeya, R., Taniguchi, K., Tanoue, Y., Tominaga, R., Sumimoto, H., 2012b. Expression and subcellular localization of mammalian formin Fhod3 in the embryonic and adult heart. PLoS One 7, e34765. https://doi.org/10.1371/journal.pone.0034765.
Katoh, M., Katoh, M., 2004. Identification and characterization of human FHOD3 gene in silico. Int. J. Mol. Med. 13, 615–620.
Keppetipola, N., Sharma, S., Li, Q., Black, D.L., 2012. Neuronal regulation of pre-mRNA splicing by polypyrimidine tract binding proteins, PTBP1 and PTBP2. Crit. Rev. Biochem. Mol. Biol. 47, 360–378. https://doi.org/10.3109/10409238.2012.691456.
Koshelev, M., Sarma, S., Price, R.E., Wehrens, X.H.T., Cooper, T.A., 2010. Heart-specific overexpression of CUGBP1 reproduces functional and molecular abnormalities of myotonic dystrophy type 1. Hum. Mol. Genet. 19, 1066–1075. https://doi.org/10.1093/hmg/ddp570.
Kühn, S., Geyer, M., 2014. Formins as effector proteins of Rho GTPases. Small GTPases 5, e29513. https://doi.org/10.4161/sgtp.29513.
Lara-Pezzi, E., Gómez-Salinero, J., Gatto, A., García-Pavía, P., 2013. The alternative heart: impact of alternative splicing in heart disease. J. Cardiovasc. Transl. Res. 6, 945–955. https://doi.org/10.1007/s12265-013-9482-z.
Latorre, E., Harries, L.W., 2017. Splicing regulatory factors, ageing and age-related disease. Ageing Res. Rev. https://doi.org/10.1016/j.arr.2017.04.004.
Li, F., Higgs, H.N., 2003. The mouse formin mDia1 is a potent actin nucleation factor regulated by autoinhibition. Curr. Biol. 13, 1335–1340.
Li, D., Morales, A., Gonzalez-Quintana, J., Norton, N., Siegfried, J.D., Hofmeyer, M., Hershberger, R.E., 2010. Identification of novel mutations in RBM20 in patients with dilated cardiomyopathy. Clin. Transl. Sci. 3, 90–97. https://doi.org/10.1111/j.1752-8062.2010.00198.x.
Li, S., Guo, W., Dewey, C.N., Greaser, M.L., 2013. Rbm20 regulates titin alternative splicing as a splicing repressor. Nucleic Acids Res. 41, 2659–2672. https://doi.org/10.1093/nar/gks1362.
Lin, X., Miller, J.W., Mankodi, A., Kanadia, R.N., Yuan, Y., Moxley, R.T., Swanson, M.S., Thornton, C.A., 2006. Failure of MBNL1-dependent post-natal splicing transitions in myotonic dystrophy. Hum. Mol. Genet. 15, 2087–2097. https://doi.org/10.1093/hmg/ddl132.
Long, J.C., Caceres, J.F., 2009. The SR protein family of splicing factors: master regulators of gene expression. Biochem. J. 417, 15–27. https://doi.org/10.1042/BJ20081501.
Maatz, H., Jens, M., Liss, M., Schafer, S., Heinig, M., Kirchner, M., Adami, E., Rintisch, C., Dauksaite, V., Radke, M.H., Selbach, M., Barton, P.J.R., Cook, S.A., Rajewsky, N., Gotthardt, M., Landthaler, M., Hubner, N., 2014. RNA-binding protein RBM20 represses splicing to orchestrate cardiac pre-mRNA processing. J. Clin. Invest. 124, 3419–3430. https://doi.org/10.1172/JCI74523.
Makeyev, E.V., Zhang, J., Carrasco, M.A., Maniatis, T., 2007. The MicroRNA miR-124 promotes neuronal differentiation by triggering brain-specific alternative pre-mRNA splicing. Mol. Cell. 27, 435–448. https://doi.org/10.1016/j.molcel.2007.07.015.
Martinez-Contreras, R., Cloutier, P., Shkreta, L., Fisette, J.-F., Revil, T., Chabot, B., 2007. hnRNP proteins and splicing control. Adv. Exp. Med. Biol. 623, 123–147.
Mirtschink, P., Krishnan, J., Grimm, F., Sarre, A., Hörl, M., Kayikci, M., Fankhauser, N., Christinat, Y., Cortijo, C., Feehan, O., Vukolic, A., Sossalla, S., Stehr, S.N., Ule, J., Zamboni, N., Pedrazzini, T., Krek, W., 2015. HIF-driven SF3B1 induces KHK-C to enforce fructolysis and heart disease. Nature 522, 444–449. https://doi.org/10.1038/nature14508.
Murayama, R., Kimura-Asami, M., Togo-Ohno, M., Yamasaki-Kato, Y., Naruse, T.K., Yamamoto, T., Hayashi, T., Ai, T., Spoonamore, K.G., Kovacs, R.J., Vatta, M., Iizuka, M., Saito, M., Wani, S., Hiraoka, Y., Kimura, A., Kuroyanagi, H., 2018. Phosphorylation of the RSRSP stretch is critical for splicing regulation by RNA-binding motif protein 20 (RBM20) through nuclear localization. Sci. Rep. 8, 8970. https://doi.org/10.1038/s41598-018-26624-w.
Nilsen, T.W., Graveley, B.R., 2010. Expansion of the eukaryotic proteome by alternative splicing. Nature 463, 457–463. https://doi.org/10.1038/nature08909.
Oberstrass, F.C., Auweter, S.D., Erat, M., Hargous, Y., Henning, A., Wenter, P., Reymond, L., Amir-Ahmady, B., Pitsch, S., Black, D.L., Allain, F.H.-T., 2005. Structure of PTB bound to RNA: specific binding and implications for splicing regulation. Science 80-(309), 2054–2057. https://doi.org/10.1126/science.1114066.
Paz, I., Kosti, I., Ares, M., Cline, M., Mandel-Gutfreund, Y., 2014. RBPmap: a web server for mapping binding sites of RNA-binding proteins. Nucleic Acids Res. 42, W361–W367. https://doi.org/10.1093/nar/gku406.
Pedrotti, S., Giudice, J., Dagnino-Acosta, A., Knoblauch, M., Singh, R.K., Hanna, A., Mo, Q., Hicks, J., Hamilton, S., Cooper, T.A., 2015. The RNA-binding protein Rbfox1 regulates splicing required for skeletal muscle structure and function. Hum. Mol. Genet. 24, 2360–2374. https://doi.org/10.1093/hmg/ddv003.
Poon, K.L., Tan, K.T., Wei, Y.Y., Ng, C.P., Colman, A., Korzh, V., Xu, X.Q., 2012. RNA-binding protein RBM24 is required for sarcomere assembly and heart contractility. Cardiovasc. Res. 94, 418–427. https://doi.org/10.1093/cvr/cvs095.
Refaat, M.M., Lubitz, S.A., Makino, S., Islam, Z., Frangiskakis, J.M., Mehdi, H., Gutmann, R., Zhang, M.L., Bloom, H.L., MacRae, C.A., Dudley, S.C., Shalaby, A.A., Weiss, R., McNamara, D.M., London, B., Ellinor, P.T., 2012. Genetic variation in the alternative splicing regulator RBM20 is associated with dilated cardiomyopathy. Hear. Rhythm 9, 390–396. https://doi.org/10.1016/j.hrthm.2011.10.016.
Rexiati, M., Sun, M., Guo, W., 2018. Muscle-specific mis-splicing and heart disease exemplified by RBM20. Genes (Basel). https://doi.org/10.3390/genes9010018.
Rinn, J.L., Kertesz, M., Wang, J.K., Squazzo, S.L., Xu, X., Brugmann, S.A., Goodnough, L.H., Helms, J.A., Farnham, P.J., Segal, E., Chang, H.Y., 2007. Functional demarcation of active and silent chromatin domains in human HOX loci by noncoding RNAs. Cell 129, 1311–1323. https://doi.org/10.1016/j.cell.2007.05.022.
Romanelli, M.G., Lorenzi, P., Morandi, C., 2000. Organization of the human gene encoding heterogeneous nuclear ribonucleoprotein type I (hnRNP I) and characterization of hnRNP I related pseudogene. Gene 255, 267–272.
Romanelli, M., Diani, E., Lievens, P., 2013. New insights into functional roles of the polypyrimidine tract-binding protein. Int. J. Mol. Sci. 14, 22906–22932. https://doi.org/10.3390/ijms141122906.
Saez, B., Walter, M.J., Graubert, T.A., 2017. Splicing factor gene mutations in hematologic malignancies. Blood 129, 1260–1269. https://doi.org/10.1182/blood-2016-10-692400.
Sahebi, M., Hanafi, M.M., van Wijnen, A.J., Azizi, P., Abiri, R., Ashkani, S., Taheri, S., 2016. Towards understanding pre-mRNA splicing mechanisms and the role of SR proteins. Gene 587, 107–119. https://doi.org/10.1016/j.gene.2016.04.057.
Schönichen, A., Geyer, M., 2010. Fifteen formins for an actin filament: a molecular view on the regulation of human formins. Biochim. Biophys. Acta 1803, 152–163. https://doi.org/10.1016/j.bbamcr.2010.01.014.
Schulze, N., Graessl, M., Blancke Soares, A., Geyer, M., Dehmelt, L., Nalbant, P., 2014. FHOD1 regulates stress fiber organization by controlling the dynamics of transverse arcs and dorsal fibers. J. Cell Sci. 127, 1379–1393. https://doi.org/10.1242/jcs.134627.
Scotti, M.M., Swanson, M.S., 2016. RNA mis-splicing in disease. Nat. Rev. Genet. 17,

19–32. https://doi.org/10.1038/nrg.2015.3.
Taniguchi, K., Takeya, R., Suetsugu, S., Kan-O, M., Narusawa, M., Shiose, A., Tominaga, R., Sumimoto, H., 2009. Mammalian formin fhod3 regulates actin assembly and sarcomere organization in striated muscles. J. Biol. Chem. 284, 29873–29881. https://doi.org/10.1074/jbc.M109.059303.
van den Hoogenhof, M.M.G., Pinto, Y.M., Creemers, E.E., 2016. RNA splicing. Circ. Res. 118, 454–468. https://doi.org/10.1161/CIRCRESAHA.115.307872.
Vuong, J.K., Lin, C.H., Zhang, M., Chen, L., Black, D.L., Zheng, S., 2016. PTBP1 and PTBP2 serve both specific and redundant functions in neuronal pre-mRNA splicing. Cell. Rep. 17, 2766–2775. https://doi.org/10.1016/j.celrep.2016.11.034.
Wagner, E.J., Garcia-Blanco, M.A., 2001. Polypyrimidine tract binding protein antagonizes exon definition. Mol. Cell. Biol. 21, 3281–3288. https://doi.org/10.1128/MCB.21.10.3281-3288.2001.
Wang, Z., Burge, C.B., 2008. Splicing regulation: from a parts list of regulatory elements to an integrated splicing code. RNA 14, 802–813. https://doi.org/10.1261/rna.876308.
Wang, G.-S., Kearney, D.L., De Biasi, M., Taffet, G., Cooper, T.A., 2007. Elevation of RNA-binding protein CUGBP1 is an early event in an inducible heart-specific mouse model of myotonic dystrophy. J. Clin. Invest. 117, 2802–2811. https://doi.org/10.1172/JCI32308.
Wang, E.T., Sandberg, R., Luo, S., Khrebtukova, I., Zhang, L., Mayr, C., Kingsmore, S.F., Schroth, G.P., Burge, C.B., 2008. Alternative isoform regulation in human tissue transcriptomes. Nature 456, 470–476. https://doi.org/10.1038/nature07509.
Waterhouse, A.M., Procter, J.B., Martin, D.M.A., Clamp, M., Barton, G.J., 2009. Jalview version 2–a multiple sequence alignment editor and analysis workbench. Bioinformatics 25, 1189–1191. https://doi.org/10.1093/bioinformatics/btp033.
Weeland, C.J., van den Hoogenhof, M.M., Beqqali, A., Creemers, E.E., 2015. Insights into alternative splicing of sarcomeric genes in the heart. J. Mol. Cell. Cardiol. 81, 107–113. https://doi.org/10.1016/j.yjmcc.2015.02.008.
Wollerton, M.C., Gooding, C., Wagner, E.J., Garcia-Blanco, M.A., Smith, C.W.J., 2004. Autoregulation of polypyrimidine tract binding protein by alternative splicing leading to nonsense-mediated decay. Mol. Cell. 13, 91–100.
Wooten, E.C., Hebl, V.B., Wolf, M.J., Greytak, S.R., Orr, N.M., Draper, I., Calvino, J.E., Kapur, N.K., Maron, M.S., Kullo, I.J., Ommen, S.R., Bos, J.M., Ackerman, M.J., Huggins, G.S., 2013. Formin homology 2 domain containing 3 variants associated with hypertrophic cardiomyopathy. Circ. Cardiovasc. Genet. 6, 10–18. https://doi.org/10.1161/CIRCGENETICS.112.965277.
Wyles, S.P., Li, X., Hrstka, S.C., Reyes, S., Oommen, S., Beraldi, R., Edwards, J., Terzic, A., Olson, T.M., Nelson, T.J., 2016. Modeling structural and functional deficiencies of *RBM20* familial dilated cardiomyopathy using human induced pluripotent stem cells. Hum. Mol. Genet. 25, 254–265. https://doi.org/10.1093/hmg/ddv468.
Xue, Y., Zhou, Y., Wu, T., Zhu, T., Ji, X., Kwon, Y.-S., Zhang, C., Yeo, G., Black, D.L., Sun, H., Fu, X.-D., Zhang, Y., 2009. Genome-wide analysis of PTB-RNA interactions reveals a strategy used by the general splicing repressor to modulate exon inclusion or skipping. Mol. Cell 36, 996–1006. https://doi.org/10.1016/j.molcel.2009.12.003.
Yang, J., Hung, L.-H., Licht, T., Kostin, S., Looso, M., Khrameeva, E., Bindereif, A., Schneider, A., Braun, T., 2014. RBM24 is a major regulator of muscle-specific alternative splicing. Dev. Cell 31, 87–99. https://doi.org/10.1016/j.devcel.2014.08.025.
Zheng, S., Gray, E.E., Chawla, G., Porse, B.T., O'Dell, T.J., Black, D.L., 2012. PSD-95 is post-transcriptionally repressed during early neural development by PTBP1 and PTBP2. Nat. Neurosci. 15, 381–388. https://doi.org/10.1038/nn.3026.
Zhou, Z., Fu, X.-D., 2013. Regulation of splicing by SR proteins and SR protein-specific kinases. Chromosoma 122, 191–207. https://doi.org/10.1007/s00412-013-0407-z.
Zhu, C., Chen, Z., Guo, W., 2017. Pre-mRNA mis-splicing of sarcomeric genes in heart failure. Biochim. Biophys. Acta - Mol. Basis Dis. 1863, 2056–2063. https://doi.org/10.1016/j.bbadis.2016.11.008.